




Article

Predictive Analysis and Wine-Grapes Disease Risk Assessment Based on Atmospheric Parameters and Precision Agriculture Platform

Ioana Marcu ¹ , Ana-Maria Drăgulescu ^{1,*} , Cristina Oprea ¹ , George Suciu ²  and Cristina Bălăceanu ² 

¹ Telecommunications Department, University Politehnica of Bucharest, 61071 Bucharest, Romania

² R&D Department, Beia Consult International, 41386 Bucharest, Romania

* Correspondence: ana.dragulescu@upb.ro

Abstract: In the precision viticulture domain, data recorded by monitoring devices are large-scale processed to improve solutions for grapes' quality and global production and to offer various recommendations to achieve these goals. Soil-related parameters (soil moisture, structure, etc.) and atmospheric parameters (precipitation, cumulative amount of heat) may facilitate crop diseases occurrence; thus, following predictive analysis, their estimation in vineyards can offer an early-stage warning for farmers and, therefore, suggestions for their prevention and treatment are of particular importance. Using remote sensing devices (e.g., satellites, unmanned vehicles) and proximal sensing methods (e.g., wireless sensor networks (WSNs)), we developed an efficient precision agriculture telemetry platform to provide reliable assessments of atmospheric phenomena periodicity and crop diseases estimation in a vineyard near Bucharest, Romania. The novelty of the materials and methods of this work relies on providing comprehensive preliminary references about monitored parameters to enable efficient, sustainable agriculture. Comparative analyses for two consecutive years illustrate an excellent correlation between cumulative and daily heat, precipitation quantity, and daily evapotranspiration (ET). In addition, the platform proved viable for wine-grapes disease estimation (powdery mildew, grape bunch rot, and grape downy mildew) and treatment recommendations based on the elaborated phenological calendar. Our results, together with continuous monitoring for the upcoming years, may be used as a reference to perform productive, sustainable smart agriculture in terms of yield and crop quality in Romania. In the Conclusion section, we show that farmers and personnel from cooperatives can use this information to make assessments based on the correlation of the available data to avoid critical damage to the wine-grape.

Keywords: IoT-WSN; precision sustainable agriculture; parameter prediction; disease estimation



Citation: Marcu, I.; Drăgulescu, A.-M.; Oprea, C.; Suciu, G.; Bălăceanu, C. Predictive Analysis and Wine-Grapes Disease Risk Assessment Based on Atmospheric Parameters and Precision Agriculture Platform. *Sustainability* **2022**, *14*, 11487. <https://doi.org/10.3390/su141811487>

Academic Editors: Michael S. Carolan, Teodor Rusu and Anup Das

Received: 3 July 2022

Accepted: 9 September 2022

Published: 13 September 2022

Publisher's Note: MDPI stays neutral with regard to jurisdictional claims in published maps and institutional affiliations.



Copyright: © 2022 by the authors. Licensee MDPI, Basel, Switzerland. This article is an open access article distributed under the terms and conditions of the Creative Commons Attribution (CC BY) license (<https://creativecommons.org/licenses/by/4.0/>).

1. Introduction

The precision agriculture domain refers to specific agricultural activities and productivity components, including the hardware and software resources used to ensure reliable (precise) results in terms of productivity yields. The overall components related to soil, air, crops, and meteorological phenomena that affect productivity and overall yield, including soil-related aspects, fertilization, the degree of contamination, dryness/excessive humidity, etc., are addressed in [1–4]. Atmospheric phenomena also bring a considerable influence over mandatory stages related to crop development and management, too. Solar energy is relevant for all stages of crop development, from seed germination to flowering/fruiting, and its effects can be either positive or negative [5–8]. Green plants use photosynthetically active radiation (PAR) for photosynthesis. PAR varies with latitude, season, clouds, etc. [9]. Regarding grapevine leaves' resistance to downy mildew (*Plasmopara viticola*), the leaves receiving 100% solar radiation should have fewer mildew problems than the shadowed leaves [6]. Solar radiation also has a significant role in evaporation and transpiration evaporation processes and, since they are interconnected, the common term to express

them is crop evapotranspiration (crop ET) [10]. Moreover, the air temperature strongly influences the type of crop that can be grown in a certain geographical area since crops have “biological clocks”. Regardless of the use-case (e.g., flowering onset time changes of alpine ginger *Roscoea*, *Ferrugem_Branca* in maize crop or wilt in sugarcane crop [5,11–13], there are crops resilient to low temperatures and others that have an efficient development in a warm environment. The ambient temperature influences the metabolism of berry grapes since elevated temperatures severely affect it, leading to low wine quality [14]. Along with air temperature, wind speed and direction, and air pressure, precipitation (daily/monthly amount) must be considered in growth prediction and disease estimation degree of grapes, and it can be classified as convective/cyclonic/frontal/orographic [15]. Precipitation has a strong influence on spreading pathogens and pests, leading to severe crop diseases in plants, including fungal diseases such as black rot (*Guignardia bidwellii*), powdery mildew (*Uncinula necator*), downy mildew, Pierce’s disease (*Xylella fastidiosa*), and Phylloxera (*Daktulosphaira vitifoliae*) [16–19]. The influence of vegetation on precipitation can be both positive and negative. The richer the vegetation, the higher the ET; thus, the amount of water in the atmosphere increases, meaning that the precipitation’s volume increases. ET is vital in water resources management and irrigation-efficient planning projects in smart cities and smart agriculture [3]. Thus, crop diseases are associated with unacceptable weather conditions and improper use of pesticides/fertilizers. Some are easily identified (diseases with distinct spectral signatures), while when multiple biotic and abiotic conditions with similar spectral characteristics are used in a cultivation area, they are more difficult to detect, if not impossible [20]. Different technologies (e.g., machine learning (ML) techniques, sensors image processing, etc. [21]) and smart systems are involved in crop disease assessment, prevention, and control. Furthermore, the global digital agriculture market grew by USD 0.6 billion from 2020 to 2021, and technologies such as Big Data, blockchain with Internet of Things (IoT) and 5G capabilities, security, and privacy solutions, provide reliability and efficiency of precision agriculture systems. IoT integration in smart farming target applications varies from typical large farming operations to organic and/or family farming, and enhances highly transparent farming [22]. The complexity of precision agriculture systems increases with the integration of wireless sensor networks (WSNs) with dedicated sensors, control systems, robotics, autonomous vehicles, automated hardware, etc. Moreover, WSNs and IoT capabilities improved the efficiency of smart agriculture systems by providing reliable parameters’ estimates such as soil and air humidity, soil and air temperature, solar radiation index, evapotranspiration, fertilizer presence, and crops development progress [23–27]. To overcome the negative effects of the ongoing climate on crops’ health, several advanced solutions were presented [28–31]. Other extensions of IoT and WSNs applications refer to the management of greenhouses and production process, monitoring and optimization of crop development in farmland, and activities related to crop protection against animal attacks [32–36].

In this context, the paper comes with the following contributions: (i) Designing, implementing, and testing a precision agriculture platform (IoT–WSN-based ADCON platform) to collect reliable and coherent data for sustainable agriculture (using predictions on atmospheric parameters and crop diseases estimation). The platform is equipped with sensors for soil and air temperature, soil and air humidity, precipitation, and solar radiation index; (ii) Visualization of different estimated values for specific parameters for wine-grapes diseases such as powdery mildew, grape bunch rot, and grapes downy mildew using the integrated platform; (iii) Proposing a methodology to analyze data (using statistical analysis) and extract valuable parameters for disease assessment to express different predictable behaviors; (iv) Presenting the phenological calendar of the monitored crop; (v) Estimating the evolution of wine-grapes diseases and the disease pressure index in terms of treatment efficiency for powdery mildew, grape bunch rot, and grape downy mildew.

To this aim, further, the paper is organized as follows: Section 2 introduces the materials and methods used for the crop (wine-grapes) monitoring and diseases prediction, including the description of our precision agriculture platform; Section 3 provides on-

field experiments, results, and discussions based on displayed tables and graphs. Finally, Section 4 is dedicated to specific conclusions based on experimental results and corresponding observations.

2. Materials and Methods

2.1. Precision Agriculture Platform

The architecture of the functional precision agriculture platform is given in Figure 1.

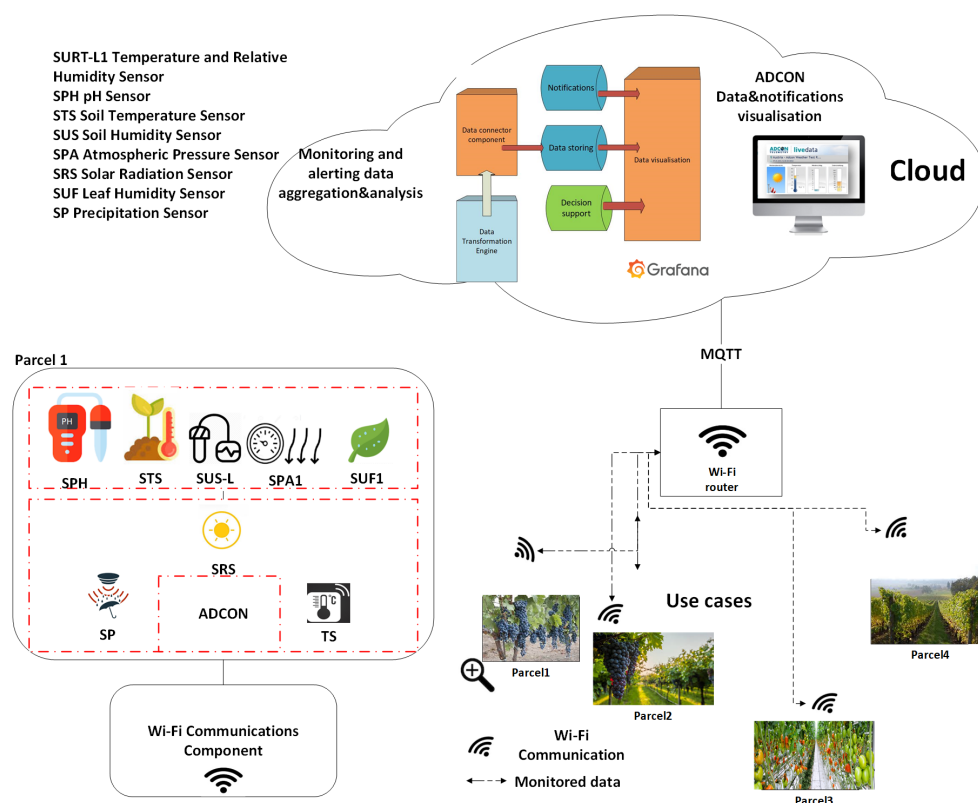


Figure 1. The architecture of the precision agriculture platform (adapted from [24,37]).

This architecture was designed and implemented as an adapted version of a previous architecture developed by the authors [24,37]. The components' interconnectivity and functionality, as well as the information flow, are depicted. Each area, called a parcel, refers to a parcel or a group of parcels, including sensing devices (agricultural dedicated sensors such as air and soil temperature, air and soil humidity, precipitation level, solar radiation, etc.). These sensors are integrated into a hardware platform equipped with a Wi-Fi communication module. For this paper, though, we will exemplify only the ADCON subcomponent of the parcel layer. For the reader to be clear that the platform also comprises other devices, we depicted the whole existing system in the development of which the team is involved.

The platform is equipped with a solar panel and battery to supply the system with the power required. The Wi-Fi communication layer ensures communication between the parcel layer and the router. Given the physical separation between the different parcels, the interval between successive transmissions, and the low interference level in the area, congestion issues do not appear and there is a small probability of data packet loss. Nevertheless, malfunctions at the power supply level (battery and solar panel) may lead to unreliable operation. This drawback is mitigated by continuously monitoring the battery level and sending a notification whenever it reaches critical levels, showing that the solar panel supply is not working correctly or that the battery recharging cycle number has been reached. Further, data are forwarded, using the Message Queueing Telemetry Transport (MQTT) protocol, to the Cloud layer, which

deals with data extraction, formatting, and storing for further decisions. These decisions consider all the parcels and the collected data.

The local Cloud component also comprises an alerting and decision support component. Grafana [38] is a very scalable open-source Cloud graphical interface used for data monitoring and additional analysis. It has many plugins and email alerts and can send notifications to beneficiaries via its interface. Each beneficiary has a dashboard with visualization panels. Behind the visualization platform, there are the databases from which the data are retrieved. In the proposed platform, we used the InfluxDB database. The data are also available through the browser-based ADCON addVANTAGE visualization platform [39], a dedicated platform for the ADCON telemetry system through which one performs data processing and data distribution. Moreover, alarms and alerts can be triggered, and disease and irrigation models can be implemented.

To conclude the relevant aspects covered by this research, a comprehensive concept for a precision agriculture framework, including key parameters, is depicted in Figure 2 [37].

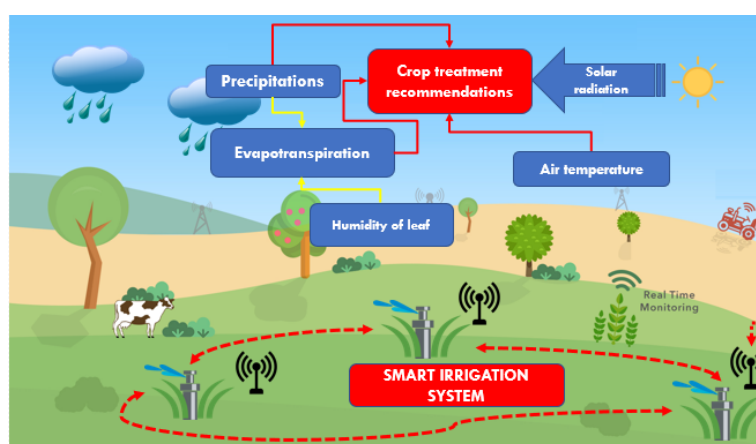


Figure 2. Key parameters in a smart agriculture framework [37].

2.2. Sensing Devices

The sensing devices (Figure 3) represent essential components of the proposed platform. Table 1 depicts those sensors of the hardware platform whose parameters were evaluated and based on which we underlie our study: air temperature sensors, precipitation sensors, and solar radiation sensors for ET determination.

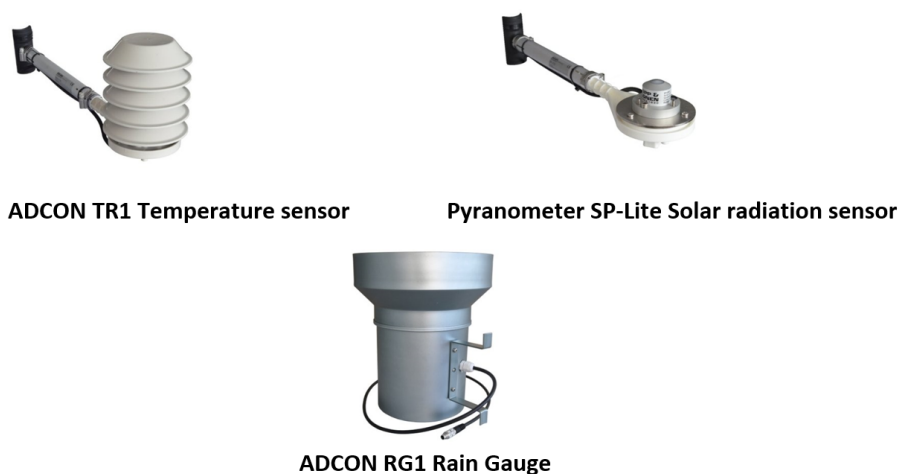


Figure 3. The sensing devices used in the proposed platform [40].

Table 1. ADCON sensors and their parameters [40].

Sensor	Parameter	Sensing Element/ Measuring Principle	Range	Accuracy/ Sensitivity
ADCON TR1	Air temperature	pt1000 DIN A	−40 °C ... +60 °C −40 °F ... +140 °F	Acc.: ±0.1 °C at 20 °C
ADCON RG1 Rain Gauge	Precipitations	Double tipping buckets	-	Acc.: up to 25 mm/h + 1%, up to 50 mm/h + 3%
Pyranometer SP-Lite	Solar radiation	Sensitive photodiode detector	Max. irradiance: 2000 W/m ²	Sens.: 75 µV/Wm ²

In addition, in Table 1, their technical characteristics are emphasized. The accuracy and sensitivity values reveal the outstanding performances of these sensing devices. The sensors are calibrated based on the calibration data stored inside the sensing device electronics [41].

2.3. Monitored Data, Methodology, and Statistics

The proposed platform is placed in a vineyard near Bucharest, Romania, in a continental climate of four seasons. We proposed and followed, for each season, a methodology to analyze the monitored data. It is split into three main parts: (i) methodology for air temperature data, (ii) methodology for precipitation data, and (iii) methodology for crop disease estimation.

2.3.1. Methodology for Air Temperature Data

- Collect air temperature data.
- Analyze the air temperature time series and eliminate the outliers based on the air temperature data range in Table 1.
- Compute the daily amount of heat (DAH) [42] based on Equation (1):

$$DAH = \frac{T_{max} + T_{min}}{2} - T_{base} \quad (1)$$

where T_{max} is the maximum temperature in a day, T_{min} is the minimum temperature in the same day, and T_{base} is the base temperature. T_{base} is the threshold temperature below which the plant stops developing. According to [43], the study using four grapevine categories and three different evaluation methods, it was predicted that T_{base} for grapes should be 10 °C (as mentioned in Table 2).

- Compute the cumulative amount of heat (CAH) [42], by adding DAH to the overall CAH parameter, as highlighted in Equation (2):

$$CAH_n = CAH_{(n-1)} + DAH \quad (2)$$

where CAH_n represents the current CAH and CAH_{n-1} represents the CAH for the previous day. For CAH, values between +10 °C and +35 °C are considered.

- Considering that crop's development is influenced by the thermal environment (temperature/heat) and that the resulting relationship typically follows a sigmoid or S-shaped curve [44], determine the parameters A, B, X_1 , and X_2 of the sigmoid curve given by Equation (3) [45] best fitting the CAH for the air temperature time series in the specific season.

$$CAH(x) = \frac{A - B}{1 + e^{\frac{x - X_1}{X_2}}} \quad (3)$$

Given the methodology for air temperature data, since crop growth and water consumption are strongly dependent on temperature, the necessary CAH for crop development is used in this paper to emphasize this process [46]. The “measurement unit” used for

CAH is growing degree days (GDDs), and its computation formula based on the maximum and minimum daily temperature is given in Equation (1) [46]. Typically, to estimate crop growing and development in the appropriate season, a specific threshold temperature must be reached and/or exceeded to facilitate this process. Thus, this threshold temperature is different for every crop and is experimentally determined and given in Table 2.

Table 2. Threshold temperatures for CAH computation [47].

Values	Crops
4.5 °C	Wheat, barley, rye, oats, lettuce, asparagus.
7.2 °C	Sunflower, potatoes.
10 °C	Sweet corn, corn, rice, grapes, soybeans, tomatoes.

Although the necessary daily temperature for a crop to grow does not vary from year to year, depending on the atmospheric conditions, DAH received by crops can vary. In addition, the GDD parameter can be computed to predict the suitability of a region for the production of a particular wine-grape variety and/or to predict the best timing of fertilizer or pesticide spread [48]. Therefore, this parameter is also represented in the experimental part of this paper.

2.3.2. Methodology for Precipitation Data

- Collect precipitations and ET data (based on solar radiation inputs) for each season.
- Analyze the precipitations time series and eliminate the outliers based on the precipitation data range in Table 1.
- Analyze the precipitation–ET balance.
- Determine precipitation autocorrelation for each season.

Finally, a comprehensive comparison between the achieved results in the years 2019 and 2020 is provided in Section 3 of this paper.

2.3.3. Methodology for Crop Diseases Estimation

Three primary diseases affecting wine-grapes production are considered for the analysis: powdery mildew, grape bunch rot, and grape downy mildew [49]. For each monitored disease, as well as for other monitored parameters, the platform has continuously monitored these parameters and issued recommendations. To achieve this, phenology aspects referring to the study of annual events in nature, events affected by seasonal changes including climate and weather, are involved in assessing disease occurrence probability. A phenological calendar is a valuable tool for communicating general climate features and the effects of climate change to the interested parties. Based on the phenological calendar estimations, the precision agriculture platform has continuously assessed the risk of significant disease occurrence due to weather conditions for the wine-grape crop. Disease pressure on leaves and berries is evaluated based on the pressure index that is real-time determined considering the probability of disease occurrence and probability of disease development based on the interaction between leaf wetness duration and temperature [50]. Interpretations of disease pressure index values are illustrated in Table 3.

Table 3. Ranges for disease pressure index [51].

Ranges for Disease Pressure Index [%]	Disease Occurrence Risk
0–30	Light risk
40–50	Moderate risk
0–100	Severe risk

Three indexes (active incubation, infection, and sporulation index) were monitored to assess GDM (Grape Downy Mildew) risk for grape downy mildew disease. Sporulation is

favorable by wet climate and warm temperatures [52]. According to [53], the infection index is a function depending on the temperature and leaf wetness duration. The correspondence between the infection index values and the risk of disease occurrence is given in Table 4.

Table 4. Ranges for infection index [53].

Ranges for Infection Index [%]	Disease Occurrence Risk
<0	No risk
0–50	Low risk
50–100	Moderate risk
100	Severe risk

Sporulation index refers to the density of spores on a leaf area and the degree of favorability of weather factors (e.g., temperature and humidity excess) [54,55]. Considering the types of sensors mounted in the monitoring system, the sporulation index determination is based on data collected by the temperature and humidity sensor [55].

For monitored diseases, preventive treatment applications are recommended when the pressure index is extremely high (a minimum of six consecutive hours is recorded for three consecutive days in which the temperature is between 20–21 °C). Time evolution of risk for each of these diseases and treatment recommendations are provided in Section 3.

3. Results and Discussion

3.1. Predictions on Atmospheric Parameters

3.1.1. Cumulative Amount of Heat (CAH)

Figure 4 illustrates the variations of CAH of heat received by grapes measured in degree-days Celsius (DC).

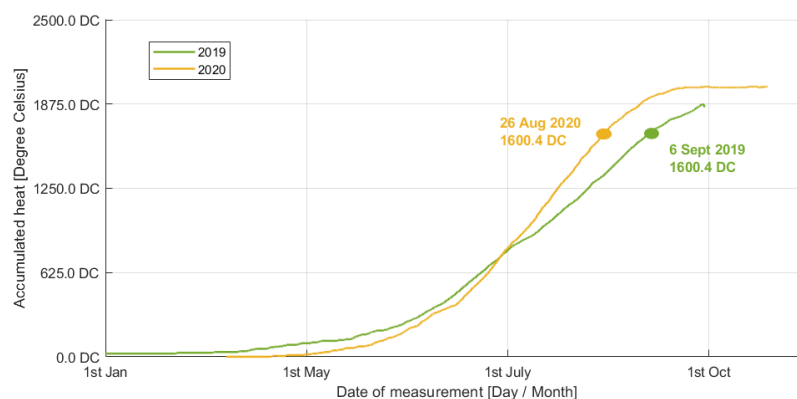


Figure 4. CAH received by grapes.

To measure this parameter, the values considered were over +10 °C, with a single value (+35 °C) for accumulated heat exceeding this limit. The appropriate value of 1600 DC (necessary for wine-grape full maturation) was measured on 6 September 2019. The same threshold was reached on 26 August 2020, meaning that farmers must consider a range of approximately two weeks when estimating the appropriate period to achieve wine-grape full maturation.

Considering the time series statistical results in 2019 and 2020, the curves that best reflect the CAH for each time series are the sigmoids given in Equation (3), with A, B, X_1 , and X_2 given in Table 5. Figure 5 reveals the results of the curve-fitting stage for the 2019 CAH data for the parameters in Table 5.

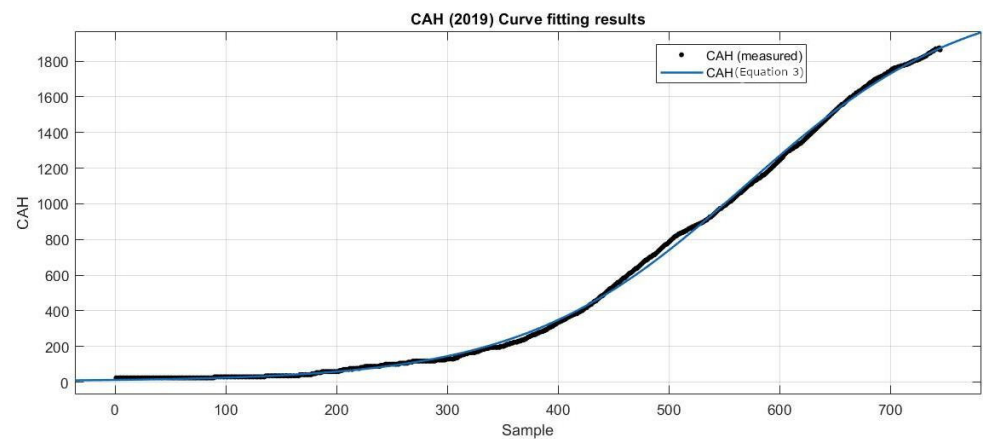


Figure 5. Curve-fitting for CAH monitored in 2019 vs. CAH determined based on Equation (3) with parameters in Table 5.

This consideration is validated by using the root mean squared error (RMSE) as a metric defined as in Equation (4). Values of RMSE closer to 0 indicate a better fitting.

$$\text{RMSE} = \sqrt{\frac{\sum_{i=1}^n w_i (y_i - \hat{y}_i)^2}{n - m}} \quad (4)$$

where n is the total number of real samples y , m is the number of fitted samples \hat{y}_i , and w_i are the weights.

We obtained RMSE = 17.46 DC for 2019 and RMSE = 24.85 DC for 2020.

Table 5. Parameters for 2019/2020 RMSE computation.

Parameter	Optimum Value		Range	
	2019	2020	2019	2020
A	4.695	−0.9744	(1.854, 7.536)	(−4.651, 2.703)
B	2195	2152	(2178, 2212)	(2146, 2157)
X_1	568.6	510.2	(566.9, 570.4)	(509.4, 511.1)
X_2	100.3	88.2	(99.23, 101.4)	(87.41, 88.98)
RMSE: 17.46 DC (2019) and RMSE: 24.85 DC (2020)				

3.1.2. The Amount of Heat Received Daily

GDD parameter predictions for best fertilizer/pesticide spread timing are based on recorded data illustrated in Figures 6 and 7.

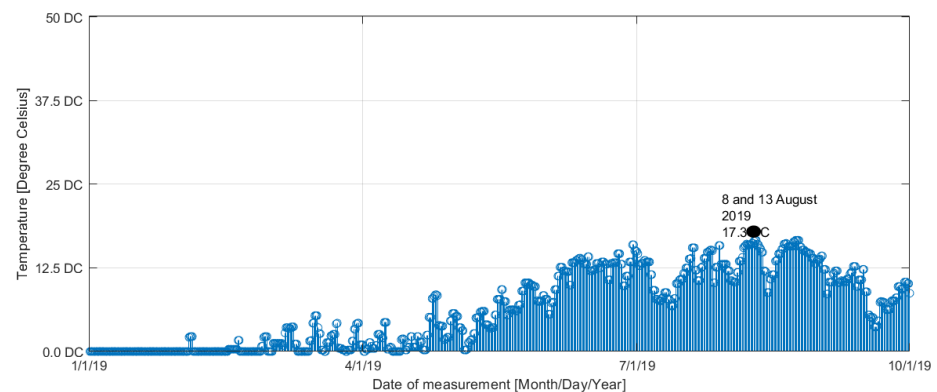


Figure 6. The daily amount of heat received by the wine-grapes (2019).

They output the permanently registered quantity of heat received daily by grapes. For example, Figure 6 shows that for 2019, the hottest 2 days were registered during 8 August and 13 August, with 17.3 DC accumulated during each of these 2 days. Using smoothing spline estimates for the daily amount of heat received by grapes in 2019, we obtained an RMSE of 0.3818 DC, for a smoothing parameter $\rho = 0.9$.

The variation for the year 2020 (Figure 7) illustrates that the warmest day was 8 August, when 20.0 DC were accumulated. For the same smoothing parameter $\rho = 0.9$, smoothing splines estimated DAH in 2020 with an RMSE = 0.631 DC, higher than in 2019.

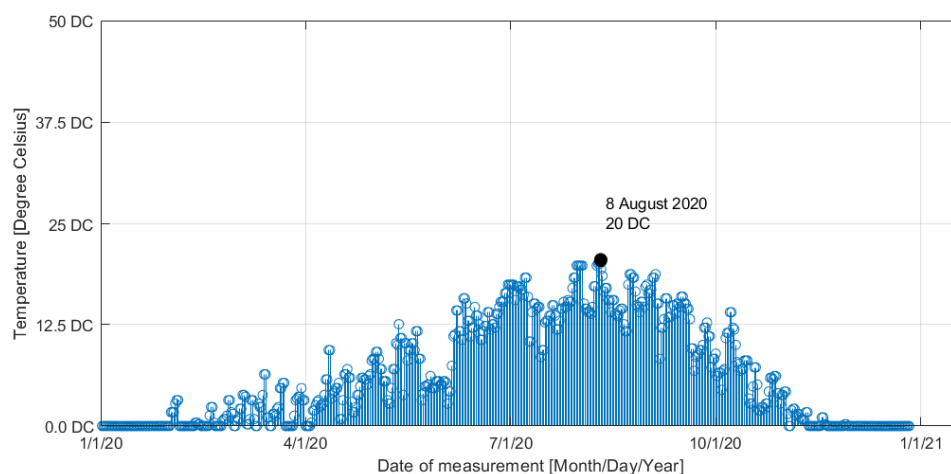


Figure 7. The daily amount of heat received by the wine-grapes (2020).

3.1.3. Precipitation

In Figures 8 and 9, the daily quantity of precipitation is represented by blue vertical bars and the crop's daily water need (crop ET) is represented by orange bars.

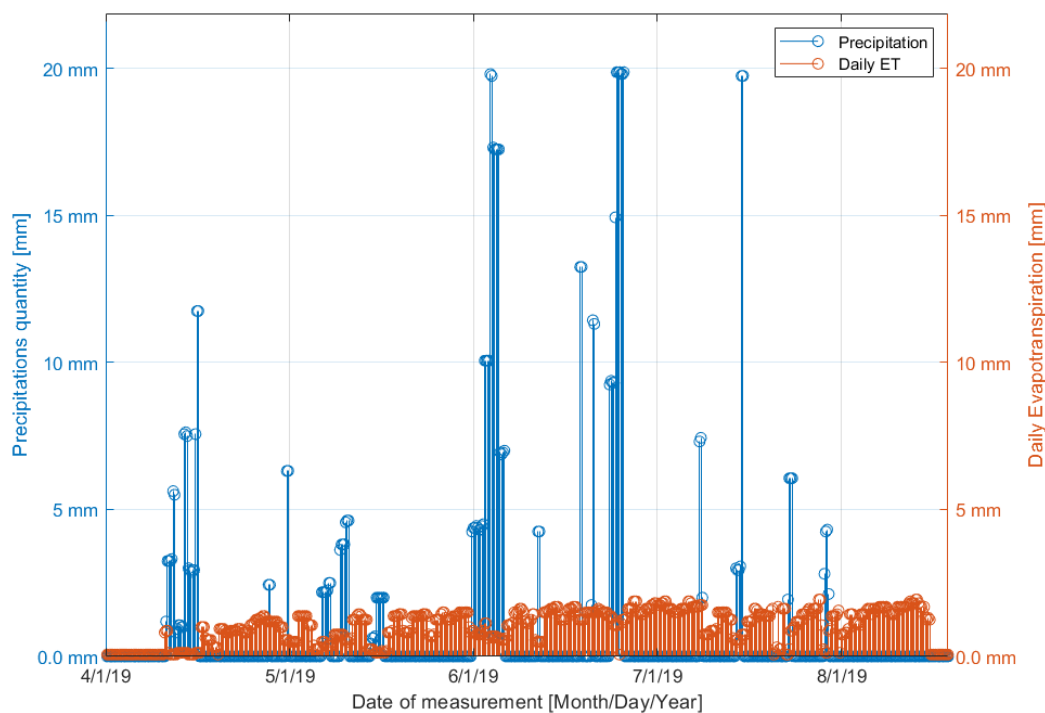


Figure 8. Precipitation quantity (2019).

For instance, on 10 May 2019, total precipitation amounted to 4.8 mm (Figure 8), while the crop ET needed was only 0.66 mm. The daily imbalance characterized the 2019

wine-growing season, in which the total precipitations exceeded the necessary amount of precipitation. For example, the total level of precipitations during June 2019 visibly exceeded the necessary amount. However, following 20 July 2019, this imbalance was reversed during the berries ripening interval. Only 12 mm of precipitation fell during this interval, considerably less than the total 41.78 mm of ET.

In an ideal model, precipitation and ET comparison level should provide information on the total amount of soil water storage, but this value also depends on other parameters, including soil texture, air temperature, etc.

The balance for the entire 2020 season of precipitation (Figure 9) compared to the crop's water needs was quite uneven, meaning that more rain occurred than necessary. Rains during May and June far exceeded the wine-grapes' need due to ET. The situation was reversed during the ripening period of the grapes, the crop receiving between 17 July 2020 and 1 September 2020 a total quantity of precipitation of only 38.0 mm, compared to the 47.52 mm that would have been needed in the first part of that period. Therefore, the summer season is equally beneficial for wine-grape growth since there are periods in which the quantity of precipitation exceeds the necessary for that period of year and periods in which precipitation lacks, and overall, the appropriate growth of berries is achieved.

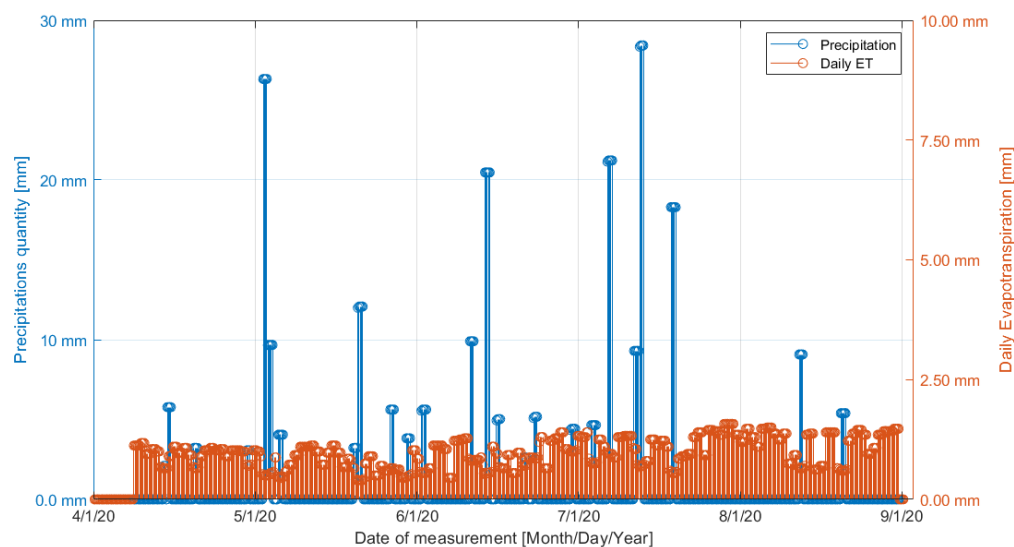


Figure 9. Precipitation quantity (2020).

Moreover, the autocorrelation of the precipitation data is relevant to detecting a periodic predictive model that can be further used to provide beneficiaries with information on the expected behavior from precipitation in a specific monitored time interval.

The autocorrelation of the 2019 and 2020 precipitation data is depicted in Figure 10 and shows a weak correlation between the samples of the experimental data for both years. Except for the 0-lag, where the autocorrelation is 1, the maximum autocorrelation for non-0-lags is 0.843 for 2019 and 0.811 for 2020, obtained for 1-lag.

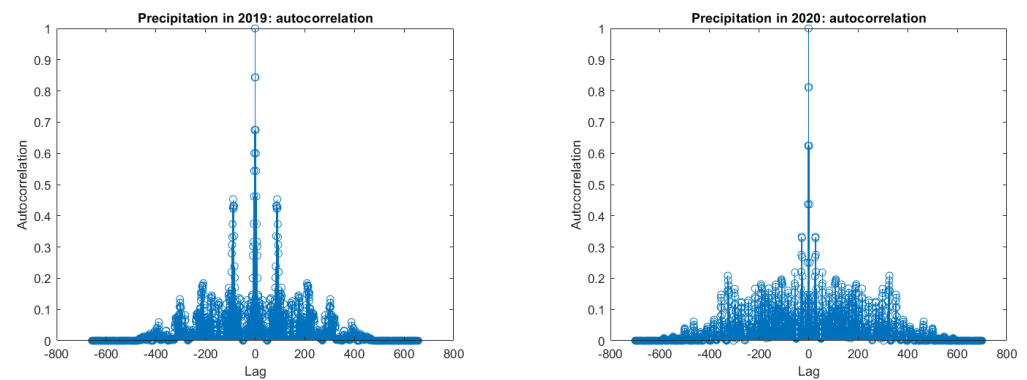


Figure 10. Precipitation quantity: autocorrelation (2019-left, 2020-right).

3.1.4. Phenological Calendar

The evolution of the accumulated heat and precipitation along the seasons (previously presented) justifies the phenological phases and, consequently, a phenological calendar was elaborated for both years 2019 and 2020 (Figure 11).

BBCH	Name	Date	
00	Winter Dormancy	Jan 1, 2019	
07	Bud Burst	Apr 10, 2019	
13	3 Leaves Unfolded	Apr 22, 2019	
55	Inflorescence Swelling	May 2, 2019	
65	Full Flowering	Jun 1, 2019	
69	End of Flowering	Jun 24, 2019	
81	Beginning of Ripening	Jul 20, 2019	
89	Berries Ripe for Harvest	Sep 6, 2019	

BBCH	Name	Date	
00	Winter Dormancy	Jan 1, 2020	
07	Bud Burst	Apr 9, 2020	
13	3 Leaves Unfolded	Apr 22, 2020	
55	Inflorescence Swelling	May 13, 2020	
65	Full Flowering	Jun 1, 2020	
69	End of Flowering	Jun 11, 2020	
81	Beginning of Ripening	Jul 24, 2020	
89	Berries Ripe for Harvest	Sep 1, 2020	

Figure 11. Phenological calendar for 2019 (left); phenological calendar for 2020 (right).

Based on Figure 11, for both monitored years, the data for each particular activity are similar, so it is intuitive and facile to make predictions regarding these stages for the next year. Therefore, the data in Figure 11 outline the reliability of the precision agriculture platform that provides valuable data for the prediction of several stages in grape growth.

3.2. Crop Diseases Estimation

Time evolution of risk for each of the monitored diseases (powdery mildew, grape bunch rot, and downy mildew), as well as treatment recommendations, are provided in this section.

3.2.1. Powdery Mildew

The evolution of the powdery mildew pressure index was continuously represented along the 2019 and 2020 seasons by the diagrams colored in orange in Figures 12 and 13.

The green line reflects the efficiency of the treatment applied against powdery mildew. The treatment efficiency is not an efficiency computed as a non-dimensional ratio between useful treatment and total treatment applied. However, it is determined by the ADCON platform, following the input by the farmer of the data associated with the performed treatment (for example, the substances used by the owner, the estimated number of days that the treatment may last). Based on the variation of temperature, humidity, and precipitation, the platform decreases or increases the number of days associated with the treatment efficiency (for example, precipitations decrease the treatment efficiency because the sprayed substances' efficiency is loosened).

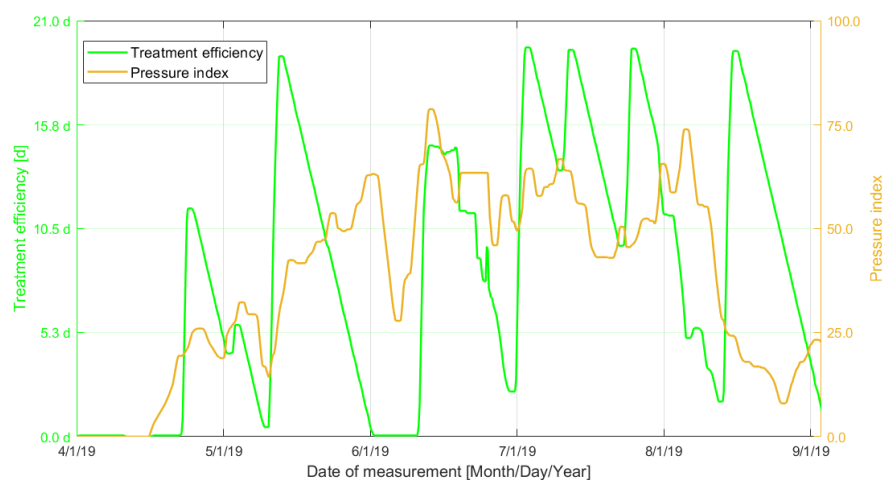


Figure 12. Powdery mildew pressure index (2019).

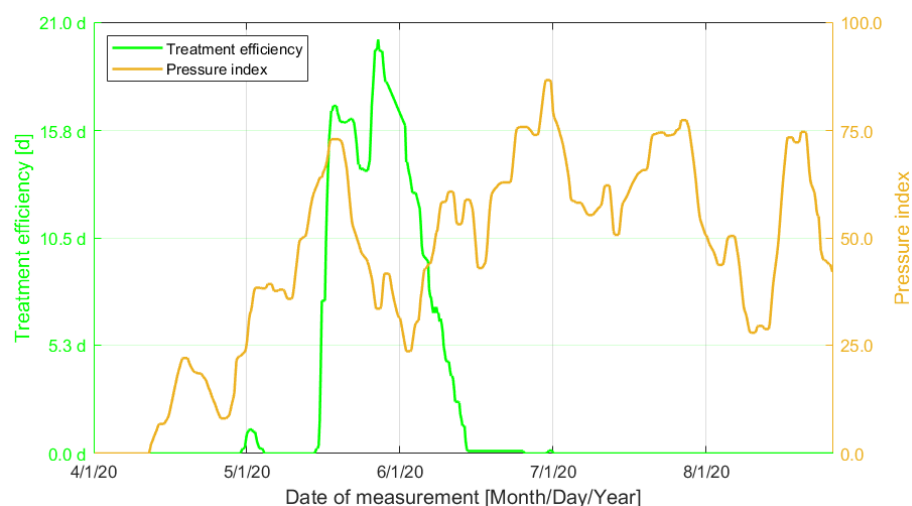


Figure 13. Powdery mildew pressure index (2020).

By correlating the information in Figures 6 and 12 (for 2019) with Figures 7 and 13 (for the year 2020), the probability of powdery mildew occurrence between the middle of June and middle of July is high due to the high DAH received by the grapes and the lack of precipitations. Therefore, on 19 June 2019, the powdery mildew pressure index reached 57.3 out of 100 units, while the treatment, previously applied around 10 June 2019, was still considered efficient for the remaining 11 days. Consequently, the two representations in Figure 12 illustrate that the powdery mildew threat was suitably addressed with treatments during the 2019 wine-growing season. A possible exception occurred during the first decade of June when abundant precipitation impeded treatment application, and the powdery mildew pressure index had the lowest value. The same observation can be made for 2020 (Figure 13), considering that on 5 June 2020, the powdery mildew index was 39.9 out of a maximum of 100 units. Therefore, the previously applied anti-flour treatment was effective for almost nine more days.

3.2.2. Grape Bunch Rot

Grape bunch rot is one of the most important diseases affecting berries. It starts with one or two berries and then spreads to the entire cluster. This disease is usually associated with a humid and wet climate. Recorded data for assessing the risk for this disease are depicted in Figure 14.

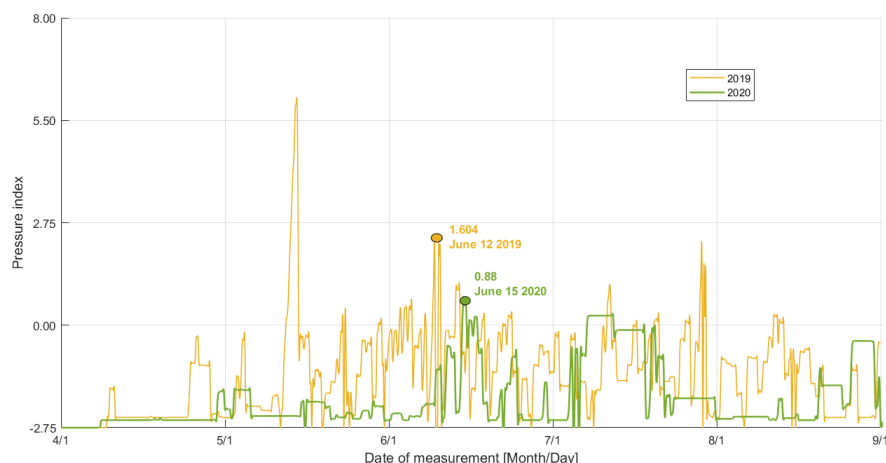


Figure 14. Grape bunch rot pressure index (2019).

According to Figure 14, the grape bunch rot threat was moderate during the 2019 and 2020 seasons because Romania does not typically have a wet and humid climate. Nevertheless, the grape bunch rot pressure index exceeded the alert limit by +0.50 in short periods (e.g., on 12 June 2019, and 15 June 2020).

3.2.3. Grape Downy Mildew

Grape downy mildew (GDM) is a severe disease for grapevines that can significantly decrease wine-grapes' yields and the quality of the harvested fruits [49].

Three indexes (active incubation, infection, and sporulation index) were monitored to assess GDM risk. Variations of these indexes (Figures 15 and 16) can only be informative and, via the platform, statistics for farmers can be provided.

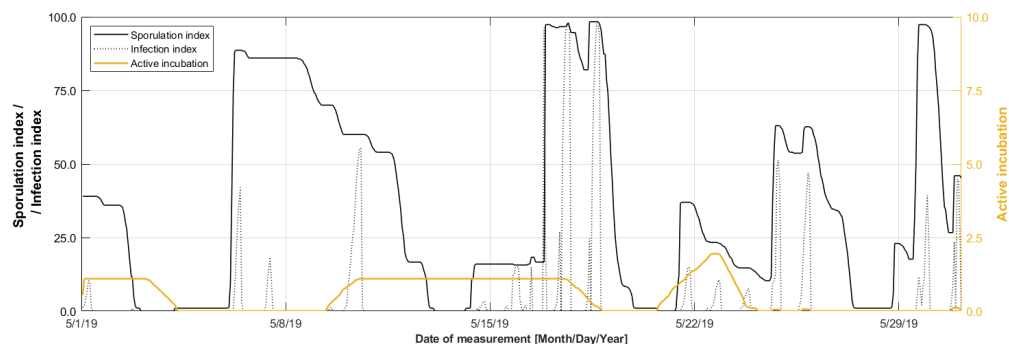
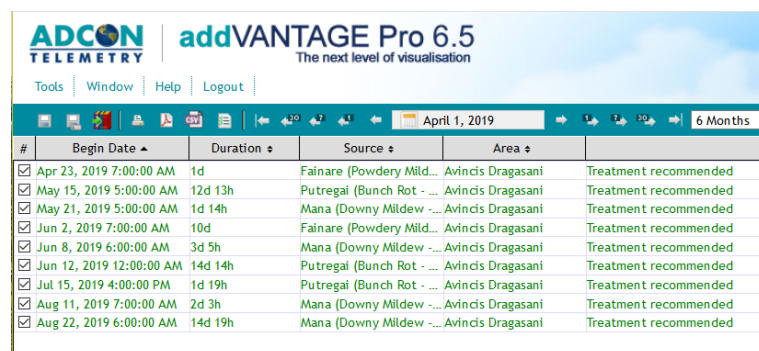


Figure 15. GDM pressure index (2019).

Sporulation is favored by wet climate and warm temperatures and, in our study, 0 represents no potential for sporulation and 100 represents highly favorable conditions for sporulation [55]. According to Figure 15, for May 2019, there are periods in which the risk of downy mildew occurrence is high (values of the index over 75), but, at the same time, this risk is not always associated with a high possibility of disease occurrence (e.g., the time intervals around 1 May, 8 May, and 30 May). However, the increase in the favorable conditions for sporulation growth leads to a higher risk of infection (e.g., the time interval around 18 May and 19 May). Similarly, increased sporulation and infection risk is not always connected to an increased active sporulation process. Consequently, although the developing stage of the spores is in the incubation period, the risk of infection and/or increased sporulation is not high. Therefore, there is no linear dependency between these three phenomena (sporulation, active sporulation, and infection indexes).

The precision agriculture platform has continuously monitored their evolutions using the Kast model [56] and has issued treatment recommendations (Figure 16).

Four treatment recommendations, dated 21 May, 8 June, 11 August, and 22 August, were issued by the system for GDM in 2019, and the system sent several e-mail alerts to the e-mail addresses contained in a predefined list. In addition, a similar GDM estimation was monitored for 2020, leading to comparable results to those in 2019.



#	Begin Date	Duration	Source	Area	
<input checked="" type="checkbox"/>	Apr 23, 2019 7:00:00 AM	1d	Fainare (Powdery Mildew)	Avincis Dragasani	Treatment recommended
<input checked="" type="checkbox"/>	May 15, 2019 5:00:00 AM	12d 13h	Putregai (Bunch Rot - ...)	Avincis Dragasani	Treatment recommended
<input checked="" type="checkbox"/>	May 21, 2019 5:00:00 AM	1d 14h	Mana (Downy Mildew - ...)	Avincis Dragasani	Treatment recommended
<input checked="" type="checkbox"/>	Jun 2, 2019 7:00:00 AM	10d	Fainare (Powdery Mildew)	Avincis Dragasani	Treatment recommended
<input checked="" type="checkbox"/>	Jun 8, 2019 6:00:00 AM	3d 5h	Mana (Downy Mildew - ...)	Avincis Dragasani	Treatment recommended
<input checked="" type="checkbox"/>	Jun 12, 2019 12:00:00 AM	14d 14h	Putregai (Bunch Rot - ...)	Avincis Dragasani	Treatment recommended
<input checked="" type="checkbox"/>	Jul 15, 2019 4:00:00 PM	1d 19h	Putregai (Bunch Rot - ...)	Avincis Dragasani	Treatment recommended
<input checked="" type="checkbox"/>	Aug 11, 2019 7:00:00 AM	2d 3h	Mana (Downy Mildew - ...)	Avincis Dragasani	Treatment recommended
<input checked="" type="checkbox"/>	Aug 22, 2019 6:00:00 AM	14d 19h	Mana (Downy Mildew - ...)	Avincis Dragasani	Treatment recommended

Figure 16. Treatment recommendation for GDM (2019).

The same variation tendency as in Figure 15 can be observed for the recorded data in May 2020 (Figure 17). The time intervals in which these indexes have a null value means that data were not recorded during that time period.

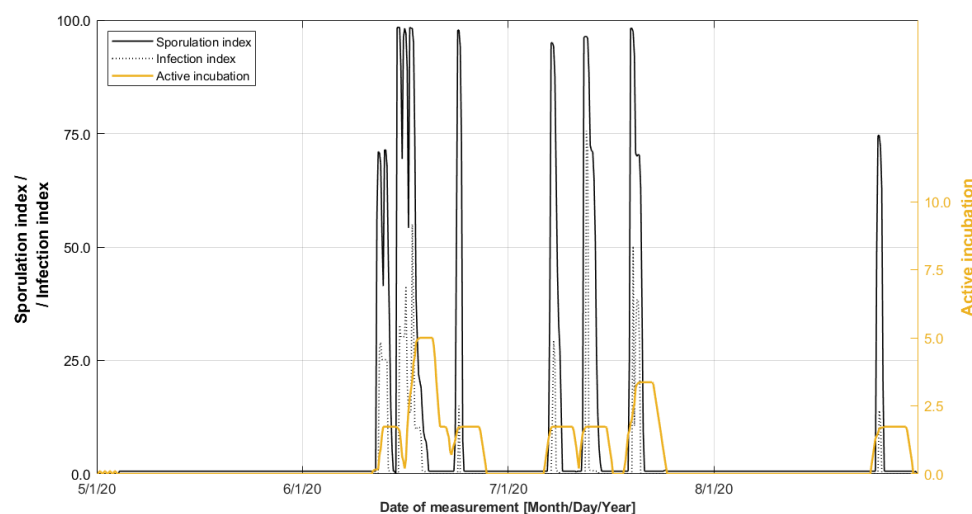


Figure 17. GDM pressure index (2020).

3.3. Discussion of Experimental Results

A comparison to similar previous analyses must be made for precise validation of our results. Nevertheless, such a requirement is difficult to accomplish since, in agricultural fields, a substantial number of parameters must be considered, such as different locations on the globe, different soil composition, and various climate conditions (variations and types). In [42], in Spain, authors determined the appropriate period for berries maturation using a maturation index and determining the heat requirements for the growth cycle starting with bud break and finishing with ripening. They conclude that, even in the open field, the maturation of the berries occurs in mid-June, compared to our estimation of August–September (Figure 4). This result is expected since Spain has diverse climate conditions depending on the geographical positioning of the territory. In France, with a climate similar to Romania, authors in [57] investigated heat requirements, phenology, and temperature data to determine the most favorable conditions for ripening. Also using

a base temperature of 10 °C, as in our study, measurement revealed that berries maturation required a higher temperature sum which is similar to our conclusion by correlating results in CAH (Figure 4) and DAH in Figures 6 and 7. In accordance with [58], by comparing results in Figures 6 and 7, we observe a global increase in daily cumulative temperature, which justifies the result for wine-grape maturation in August 2020 compared to September 2019. Daily evapotranspiration is considered for analysis in [59] in case of mitigating the heat negative effects, and the indirect effect of high temperatures causes an increase in this parameter. Correlated with data in Figures 4, 6 and 7, ET parameters in Figures 8 and 9 have significant values from April to September (time period in which the temperatures are increased). Since global warming, including extremely high temperatures and drought, is mainly responsible for precipitation quantity reduction [60,61], the same tendency can be noticed in Figures 8 and 9.

Diseases index determination and treatment recommendations in viticulture strongly depend on the climate and the specific of the grapes. For example, powdery mildew and downy mildew are considered in [62], and the authors of this report mention that the latter imposes at least 12 treatments per season in France. Similarly, due to a similar climate in Romania, Figure 16 illustrates that in six months of monitoring, most treatment recommendations are for downy mildew.

A brief conclusion of this subsection outlines that the results achieved in this study are in total agreement with other similar results obtained in countries with similar climates. Differences in variations may occur due to different climates and soil compositions.

4. Conclusions

Precision agriculture consists of critical features, parameters, technologies, strategies, and solutions for efficient crop and fruit growth and development. These are influenced by numerous phenomena, including agricultural (e.g., soil) and atmospheric (solar energy, air and soil temperature, leaf wetness, air and soil humidity, precipitation). Efforts in this domain are oriented towards efficiency and reduction of negative impact on productivity and yield, and several adopted strategies manage to mitigate such risks. The present paper introduces a precision agriculture platform equipped with dedicated agricultural sensors that continuously record and broadcast data related to critical parameters for precision agriculture.

The originality of the paper is manifold. Not only are the proposed architecture and the data collection crucial, but so are the conjunction between them and the proposed methods to analyze the data gathered from the sensors. We highlight here the methodologies for air temperature data, precipitation data, and crop disease estimation. The entire paper can guide viticulture and IT&C stakeholders through the common goal of developing precision viticulture IoT platforms that really contribute to crop disease estimation. With respect to other platforms, ours combines academic and industry experience and it is based on mature, on-field, extensive tested technologies well known in this research area (e.g., calibrated sensors, remote terminal units, communication modules, databases, decision support modules, notification components, visualization tools).

Based on the proposed methodologies and results, sustainable agriculture can be performed in this area using the implemented telemetry system. Data recorded and presented for 2019 and 2020 are a good reference for future years. The sigmoid equation to model the CAH data and the optimum parameters of this model were provided in this analysis. For the daily amount of heat, we used smoothing splines as proper estimates. Crops' disease risk assessment (powdery mildew, grape bunch rot, and grape downy mildew) is outlined, and the system's efficiency is demonstrated by the prompt option for treatment recommendation and by real-time alerting email sent to interested parties.

It would have been efficient to make a comparison with previous works developed in the same area and under the same conditions, but so far, there is no such current available work. Therefore, future work refers to expanding the system's capabilities for recording and transmitting more data related to other specific parameters for precision agriculture

(using custom sensors and technologies), and also expanding the services offered for other types of diseases that can affect other crops. Nevertheless, the parcel monitoring and analysis will be continued to obtain a relevant database for this specific crop to compare the results currently obtained with future analyses.

Author Contributions: I.M. and G.S.—conceptualization, writing—original draft; I.M., A.-M.D. and C.O.—writing—review and editing; I.M.—funding acquisition and supervision; A.-M.D. and C.O.—data curation; A.-M.D.—methodology; C.O.—software; G.S. and C.B.—resources and investigation. All authors have read and agreed to the published version of the manuscript.

Funding: This work was supported by a grant of the Romanian Ministry of Education and Research, CCCDI—UEFISCDI, project number PN-III-P2-2.1-PED-2019-1945 (NGI-UAV-AGRO) and by SmartA-gro project subsidiary contract no. 8592/08.05.2018, from the NETIO project ID: P_40_270, MySmis Code: 105976.

Institutional Review Board Statement: Not applicable.

Informed Consent Statement: Not applicable.

Data Availability Statement: The data that support the findings of this study are available from the corresponding author, A.-M.D. upon reasonable request.

Conflicts of Interest: The authors declare no conflict of interest.

Abbreviations

The following abbreviations are used in this manuscript:

CAH	Cumulative amount of heat
DAH	Daily amount of heat
DC	Degree-days Celsius
ET	Evapotranspiration
GDD	Growing degree day
GDM	Grape downy mildew
IoT	Internet of Things
ML	Machine learning
MQTT	Message Queueing Telemetry Transport
PAR	Photosynthetically active radiation
RMSE	Root mean squared error
WSNs	Wireless sensor networks

References

1. Mallarino, A. Available online: <https://crops.extension.iastate.edu/encyclopedia/using-precision-agriculture-improve-soil-fertility-management-and-farm-research> (accessed on 19 November 2021).
2. Orsini, R.; Fiorentini, M.; Zenobi, S. Evaluation of Soil Management Effect on Crop Productivity and Vegetation Indices Accuracy in Mediterranean Cereal-Based Cropping Systems. *Sensors* **2020**, *20*, 3383. [CrossRef] [PubMed]
3. Tehen, A.K.; Helming, K.; Brüggemann, N.; Veldkamp, E.; Reinhold-Hurek, B.; Lorenz, M.; Bartke, S.; Heinrich, U.; Amelung, W.; Augustin, K.; et al. Chapter Four—Soil research challenges in response to emerging agricultural soil management practices. In *Advances in Agronomy*; Academic Press: Cambridge, MA, USA, 2020; Volume 161, pp. 179–240. [CrossRef]
4. Vrindts, E.; Reyniers, M.; Darius, P.; De baerdemaeker, J.; Gilot, M.; Sadaoui, Y.; Frankinet, M.; Hanquet, B.; Destain, M.F. Analysis of Soil and Crop Properties for Precision Agriculture for Winter Wheat. *Biosyst. Eng.* **2003**, *85*, 141–152. [CrossRef]
5. Tropical Rust. Available online: <https://plantix.net/en/library/plant-diseases/100101/tropical-rust> (accessed on 24 November 2021).
6. Marta, A.D.; Stefano, V.D.; Cerovic, Z.G.; Agati, G.; Orlandini, S. Solar radiation affects grapevine susceptibility to Plasmopara Viticola. *Sci. Agric.* **2008**, *65*, 65–70. [CrossRef]
7. Ishimaru, T.; Sasaki, K.; Nozaki, I.; Ichihashi, M.; Shimizu, H.; Wakayama, M.; Hirabayashi, H. Effect of the light and dark conditions on flower opening time between cultivated rice (*Oryza Sativa*) A Near-Isogenic Early-Morning Flower Line. *AoB Plants* **2021**, *13*, plab040. [CrossRef] [PubMed]
8. Young, H.M.; George, S.; Narváez, D.F.; Srivastava, P.; Schuerger, A.C.; Wright, D.L.; Marois, J.J. Effect of Solar Radiation on Severity of Soybean Rust. *Phytopathology* **2012**, *102*, 794–803. [CrossRef] [PubMed]

9. Rabbi, B.; Chen, Z.H.; Sethuvenkatraman, S. Protected Cropping in Warm Climates: A Review of Humidity Control and Cooling Methods. *Energies* **2019**, *12*, 2737. [\[CrossRef\]](#)
10. Campillo, C.; Fortes, R.; del Henar Prieto, M. Solar Radiation Effect on Crop Production. In *Solar Radiation*; InTech: New York, NY, USA, 2012. [\[CrossRef\]](#)
11. Mohandass, D.; Zhao, J.L.; Xia, Y.M.; Campbell, M.J.; Li, Q.J. Increasing temperature causes flowering onset time changes of alpine ginger *Roscoea* in the Central Himalayas. *J. Asia-Pac. Biodivers.* **2015**, *8*, 191–198. [\[CrossRef\]](#)
12. Manavalan, R. Efficient Detection of Sugarcane Diseases through Intelligent Approaches: A Review. *Asian J. Res. Rev. Agric.* **2021**, *3*, 27–37.
13. Velásquez, A.C.; Castroverde, C.D.M.; He, S.Y. Plant–Pathogen Warfare under Changing Climate Conditions. *Curr. Biol.* **2018**, *28*, R619–R634. [\[CrossRef\]](#)
14. Venios, X.; Korkas, E.; Nisiotou, A.; Banilas, G. Grapevine Responses to Heat Stress and Global Warming. *Plants* **2020**, *9*, 1754. [\[CrossRef\]](#)
15. Vegetation Influence on Precipitation. Available online: <https://forestrypedia.com/vegetation-influence-on-precipitation/> (accessed on 19 December 2021).
16. Heuvel, J.V.; Centinari, M. Under-Vine Vegetation Mitigates the Impacts of Excessive Precipitation in Vineyards. *Front. Plant Sci.* **2021**, *12*, 1542. [\[CrossRef\]](#)
17. Hazelrigg, A.L.; Bradshaw, T.L.; Maia, G.S. Disease Susceptibility of Interspecific Cold-Hardy Grape Cultivars in Northeastern U.S.A. *Horticulturae* **2021**, *7*, 216. [\[CrossRef\]](#)
18. Du, F.; Deng, W.; Yang, M.; Wang, H.; Mao, R.; Shao, J.; Fan, J.; Chen, Y.; Fu, Y.; Li, C.; et al. Protecting grapevines from rainfall in rainy conditions reduces disease severity and enhances profitability. *Crop Prot.* **2015**, *67*, 261–268. [\[CrossRef\]](#)
19. 7 Most Common Grapevine Diseases. Available online: <https://learn.winecoolerdirect.com/common-grapevine-diseases/> (accessed on 19 December 2021).
20. Yang, C. Remote Sensing and Precision Agriculture Technologies for Crop Disease Detection and Management with a Practical Application Example. *Engineering* **2020**, *6*, 528–532. [\[CrossRef\]](#)
21. Bischoff, V.; Farias, K.; Menzen, J.P.; Pessin, G. Technological support for detection and prediction of plant diseases: A systematic mapping study. *Comput. Electron. Agric.* **2021**, *181*, 105922. [\[CrossRef\]](#)
22. The Digitisation of the European Agricultural Sector. Available online: <https://digital-strategy.ec.europa.eu/en/policies/digitisation-agriculture> (accessed on 19 November 2021).
23. Zervopoulos, A.; Tsipis, A.; Alvanou, A.G.; Bezas, K.; Papamichail, A.; Vergis, S.; Styliadou, A.; Tsoumanis, G.; Komianos, V.; Koufoudakis, G.; et al. Wireless Sensor Network Synchronization for Precision Agriculture Applications. *Agriculture* **2020**, *10*, 89. [\[CrossRef\]](#)
24. Balaceanu, C.M.; Marcu, I.; Suci, G. Telemetry System for Smart Agriculture. In *Business Information Systems Workshops*; Springer International Publishing: Cham, Switzerland, 2019; pp. 573–584. [\[CrossRef\]](#)
25. Lu, W.; Xu, X.; Huang, G.; Li, B.; Wu, Y.; Zhao, N.; Yu, F.R. Energy Efficiency Optimization in SWIPT Enabled WSNs for Smart Agriculture. *IEEE Trans. Ind. Inform.* **2021**, *17*, 4335–4344. [\[CrossRef\]](#)
26. Suci, G.; Marcu, I.; Balaceanu, C.; Dobrea, M.; Botezat, E. Efficient IoT system for Precision Agriculture. In Proceedings of the 2019 15th International Conference on Engineering of Modern Electric Systems (EMES), Oradea, Romania, 13–14 June 2019; pp. 173–176. [\[CrossRef\]](#)
27. Visconti, P.; de Fazio, R.; Velázquez, R.; Del-Valle-Soto, C.; Giannoccaro, N.I. Development of Sensors-Based Agri-Food Traceability System Remotely Managed by a Software Platform for Optimized Farm Management. *Sensors* **2020**, *20*, 3632. [\[CrossRef\]](#)
28. Food and Agriculture Organization of the United Nations. Approaches Used to Investigate the Effects of Climate Change on Plant Pests. Available online: <https://www.fao.org/3/cb4769en/online/src/html/approaches-used-to-investigate-the-effects-of-climate-change-on-plant-pests.html> (accessed on 14 January 2022).
29. Zayan, S.A. Impact of Climate Change on Plant Diseases and IPM Strategies. In *Plant Diseases—Current Threats and Management Trends*; IntechOpen: New York, NY, USA, 2020. [\[CrossRef\]](#)
30. Wang, X.; Liu, J.; Zhu, X. Early real-time detection algorithm of tomato diseases and pests in the natural environment. *Plant Methods* **2021**, *17*, 43. [\[CrossRef\]](#)
31. Newlands, N.K. Model-Based Forecasting of Agricultural Crop Disease Risk at the Regional Scale, Integrating Airborne Inoculum, Environmental, and Satellite-Based Monitoring Data. *Front. Environ. Sci.* **2018**, *6*, 63. [\[CrossRef\]](#)
32. Ravindra, S. IoT Applications in Agriculture. Available online: <https://www.iotforall.com/iot-applications-in-agriculture> (accessed on 19 December 2021).
33. Akhtar, M.N.; Shaikh, A.J.; Khan, A.; Awais, H.; Bakar, E.A.; Othman, A.R. Smart Sensing with Edge Computing in Precision Agriculture for Soil Assessment and Heavy Metal Monitoring: A Review. *Agriculture* **2021**, *11*, 475. [\[CrossRef\]](#)
34. Bu, F.; Wang, X. A smart agriculture IoT system based on deep reinforcement learning. *Future Gener. Comput. Syst.* **2019**, *99*, 500–507. [\[CrossRef\]](#)
35. Haseeb, K.; Din, I.U.; Almogren, A.; Islam, N. An Energy Efficient and Secure IoT-Based WSN Framework: An Application to Smart Agriculture. *Sensors* **2020**, *20*, 2081. [\[CrossRef\]](#) [\[PubMed\]](#)
36. Thakur, D.; Kumar, Y.; Kumar, A.; Singh, P.K. Applicability of Wireless Sensor Networks in Precision Agriculture: A Review. *Wirel. Pers. Commun.* **2019**, *107*, 471–512. [\[CrossRef\]](#)

37. Marcu, I.M.; Suciu, G.; Balaceanu, C.M.; Banaru, A. IoT based System for Smart Agriculture. In Proceedings of the 2019 11th International Conference on Electronics, Computers and Artificial Intelligence (ECAI), Pitesti, Romania, 27–29 June 2019. [CrossRef]
38. Grafana Labs. Grafana: The Open Observability Platform. Available online: <https://grafana.com/> (accessed on 12 December 2021).
39. ADCON. ADCON addVANTAGE 6.x. Available online: <https://www.adcon.com/products/software-285/adcon-addvantage-6x-1485/> (accessed on 10 September 2021).
40. ADCON. Sensors. Available online: <https://www.adcon.com/products/sensors-284/> (accessed on 10 September 2021).
41. ADCON. Available online: <https://www.adcon.com/download/leaflet-tr1-temperature-humidity-sensor/> (accessed on 19 June 2021).
42. Alonso, F.; Chiamolera, F.M.; Hueso, J.J.; González, M.; Cuevas, J. Heat Unit Requirements of “Flame Seedless” Table Grape: A Tool to Predict Its Harvest Period in Protected Cultivation. *Plants* **2021**, *10*, 904. [CrossRef]
43. Zapata, D.; Salazar, M.; Chaves, B.; Keller, M.; Hoogenboom, G. Estimation of the base temperature and growth phase duration in terms of thermal time for four grapevine cultivars. *Int. J. Biometeorol.* **2015**, *59*, 1771–1781. [CrossRef]
44. Brown, P. Heat Units. Available online: <https://cals.arizona.edu/crop/cotton/cropmgt/az1602.pdf> (accessed on 20 December 2021).
45. Lespinard, A.R.; Salgado, P.R.; Mascheroni, R.H. Sigmoid Model: Application to Heat Transfer in Vegetable Preserves Sterilized in Glass Jars. *Lat. Am. Appl. Res.* **2008**, *38*, 273–278.
46. de Medeiros, G.A.; Daniel, L.A.; Fengler, F.H. Growth, Development, and Water Consumption of Irrigated Bean Crop Related to Growing Degree-Days on Different Soil Tillage Systems in Southeast Brazil. *Int. J. Agron.* **2016**, *2016*, 1–7. [CrossRef]
47. Parthasarathi, T.; Velu, G.; Jeyakumar, P. Impact of Crop Heat Units on Growth and Developmental Physiology of Future Crop Production: A Review. *Res. Rev. J. Crop Sci. Technol.* **2013**, *2*, 2319–3395.
48. Urska. Why the Need to Calculate Growing Degree Days in Vineyard? Available online: <https://www.evinyardapp.com/blog/2017/03/01/why-the-need-to-calculate-growing-degree-days-in-vineyard/> (accessed on 19 December 2021).
49. Oliver, S.T.; González-Pérez, A.; Guijarro, J.H. Adapting Models to Warn Fungal Diseases in Vineyards Using In-Field Internet of Things (IoT) Nodes. *Sustainability* **2019**, *11*, 416. [CrossRef]
50. VitiSolutions. Development of Regional IPM Best Practice. Available online: <https://www.wineaustralia.com/getmedia/30ce63d5-57fb-4a65-a618-a9b711f6b546/VTs-06-01-Final-Report> (accessed on 21 November 2021).
51. de Oliveira, A.F.; Serra, S.; Ligios, V.; Satta, D.; Nieddu, G. Assessing the Effects of Vineyard Soil Management on Downy and Powdery Mildew Development. *Horticulturae* **2021**, *7*, 209. [CrossRef]
52. Jaspers, M.V.; Seyb, A.M.; Trought, M.C.T.; Balasubramaniam, R. Overwintering grapevine debris as an important source of *Botrytis cinerea* inoculum. *Plant Pathol.* **2013**, *62*, 130–138. [CrossRef]
53. Shah, N.G.; Desai, U.B.; Das, I.; Merchant, S.N.; Yadav, S.S. In-field wireless sensor network (WSN) for estimating evapotranspiration and leaf wetness. *Int. Agric. Eng. J.* **2009**, *18*, 43–51.
54. Coertze, S.; Holz, G.; Sadie, A. Germination and Establishment of Infection on Grape Berries by Single Airborne Conidia of *Botrytis Cinerea*. *Plant Dis.* **2001**, *85*, 668–677. [CrossRef]
55. PRISME Cosortium. Available online: <https://ipmsymposium.org/2021/Documents/PRISMECosortium.pdf> (accessed on 20 June 2022).
56. Pertot, I.; Caffi, T.; Rossi, V.; Mugnai, L.; Hoffmann, C.; Grando, M.; Gary, C.; Lafond, D.; Duso, C.; Thiery, D.; et al. A critical review of plant protection tools for reducing pesticide use on grapevine and new perspectives for the implementation of IPM in viticulture. *Crop Prot.* **2017**, *97*, 70–84. [CrossRef]
57. Van Leeuwen, C.; Garnier, C.; Agut, C.; Baculat, B.; Barbeau, G.; Besnard, E.; Bois, B.; Boursiquot, J.M.; Chuine, I.; Dessup, T.; Dufourcq, T. Heat requirements for grapevine varieties is essential information to adapt plant material in a changing climate. In Proceedings of the 2008 VIIth International terroir Congress, Agroscope Changins-Wädenswil, Nyon, Switzerland, 19–23 May 2008.
58. Droulia, F.; Charalampopoulos, I. A Review on the Observed Climate Change in Europe and Its Impacts on Viticulture. *Atmosphere* **2022**, *13*, 837. [CrossRef]
59. Martínez-Lüscher, J.; Chen, C.C.L.; Brillante, L.; Kurtural, S.K. Mitigating Heat Wave and Exposure Damage to “Cabernet Sauvignon” Wine Grape With Partial Shading Under Two Irrigation Amounts. *Front. Plant Sci.* **2020**, *11*, 579192. [CrossRef]
60. Ohba, M. Precipitation under climate change. In *Precipitation*; Elsevier: Amsterdam, The Netherlands, 2021; pp. 21–51. [CrossRef]
61. Caian, M.; Georgescu, F.; Dobre, A.; Neague, P. Variability of Precipitation in Romania: Recent Trends and Projected Changes in Climate Scenarios. WeADL 2021 Workshop. 2021. Available online: <http://www.cs.ubbcluj.ro/weadl/wp-content/uploads/2022/06/Mihaela%20Caian%20-%20Variability%20of%20precipitation%20in%20Romania.pdf> (accessed on 18 January 2022).
62. EIP-AGRI Focus Group. Diseases and Pests in Viticulture. Available online: https://ec.europa.eu/eip/agriculture/sites/default/files/eip-agri_fg_diseases_and_pests_in_viticulture_final_report_2019_en.pdf (accessed on 8 July 2022).